

Axial and diffusion models of the laser pulse propagation in a highly-scattering medium

S.A. Tereshchenko, A.A. Danilov, V.M. Podgaetskii, N.S. Vorob'ev

Abstract. The propagation of laser radiation through a layer of a highly-scattering medium (HSM) is considered on the basis of two theoretical models: a nonstationary axial (two-flux) model and a nonstationary diffusion model. Analytic expressions for the temporal distributions of the photons of an ultrashort laser pulse transmitted through the HSM are presented. Experimental temporal distributions are used to obtain the parameters of models corresponding to an HSM, to determine the theoretical temporal distributions, and to compare them with the experimental curves. These two theoretical models are compared quantitatively for the first time. Their advantages and drawbacks that must be considered in the development of HSM transmission optical tomography are pointed out.

Keywords: highly-scattering medium, optical tomography, ultrashort pulse, interaction of radiation with matter.

1. Formulation of the problem

The problem of developing transmission optical tomography of a highly-scattering medium (HSM), to which biological tissues also belong, has been attracting considerable attention of the international scientific community for more than ten years [1–4]. Nevertheless, this problem cannot be considered solved so far because the interaction of optical radiation with a HSM is governed by complex processes. These processes are described using the radiation transfer equation (RTE) [5–7] that takes scattering into account. At present, the RTE is regarded as the most adequate equation for describing the propagation of radiation in a HSM. This difficult problem has actually developed into an independent direction of investigation, in which a transition to tomography is only implied.

In contrast to the RTE for a purely absorbing medium, the RTE for an HSM includes the differential (with respect to angles) radiation-scattering coefficient (the spatially nonuniform scattering indicatrix). Therefore, already two unknown functions are to be reconstructed in the trans-

mission optical tomography. Since it is impossible within the conventional tomographic scheme because of a lack of information, various approaches are used to increase the amount of the initial information. The two main approaches are:

(1) the use of a high-frequency modulation of cw laser radiation and detection of the HSM-transmitted radiation at several modulation frequencies (frequency-domain tomography);

(2) the use of laser pulse radiation and detection of the temporal distribution of the HSM-transmitted radiation (time-domain tomography).

The methods used to detect the transmitted radiation can also be divided into two groups: (i) radiation detection only on the axis of the primary beam and utilisation of two-dimensional tomographic algorithms and (ii) radiation detection at several points (ideally, at each point of the object's surface) and utilisation of three-dimensional tomographic algorithms.

In the time-domain tomography and for the radiation detection on the beam axis, it is important to study the propagation of optical radiation through a homogeneous HSM layer. As is known, photons transmitted through such a layer can be divided into two parts: the photons moving along the initial-beam direction (paraxial) and scattered (off-axial) photons moving in different directions. The paraxial photons in turn consist of photons transmitted through the medium without interacting with it (ballistic photons) and scattered photons.

The use of the RTE for describing the propagation of photons through the HSM is impeded by the fact that the RTE generally has no analytic solution. The main trend in overcoming this difficulty is the development of an intermediate simpler mathematical model based on a simplification of the RTE under additional assumptions. A diffusion model [5–7] is most frequently used in the development of transmission optical tomography. Another promising model is a nonstationary axial (two-flux) model [8]. Although these models have been studied independently and quite comprehensively, they have not been compared to each other up to now. In this paper, these two models of laser-pulse propagation through a homogeneous HSM layer are compared theoretically and experimentally.

2. Theory

The main tool for describing the interaction between radiation and matter is the RTE that can be written in the form

S.A. Tereshchenko, A.A. Danilov, V.M. Podgaetsky Moscow State Institute of Electronic Engineering (Technical University), 124498 Moscow, Zelenograd, Russia;

N.S. Vorob'ev A.M. Prokhorov General Physics Institute, Russian Academy of Sciences, ul. Vavilova 38, 119991 Moscow, Russia

Received 23 December 2003; revision received 10 March 2004

Kvantovaya Elektronika 34 (6) 541–544 (2004)

Translated by A.S. Seferov

$$S(\mathbf{r}, \mathbf{\Omega}, t) = \frac{1}{v} \frac{\partial}{\partial t} \Phi(\mathbf{r}, \mathbf{\Omega}, t) + \mathbf{\Omega} \text{grad} \Phi(\mathbf{r}, \mathbf{\Omega}, t) + \mu(\mathbf{r}) \Phi(\mathbf{r}, \mathbf{\Omega}, t) - \int_{4\pi} \Phi(\mathbf{r}, \mathbf{\Omega}', t) \mu_s(\mathbf{r}, \mathbf{\Omega}' \rightarrow \mathbf{\Omega}) d\Omega', \quad (1)$$

where $S(\mathbf{r}, \mathbf{\Omega}, t)$ is the density of the photon sources moving in direction $\mathbf{\Omega}$ at point \mathbf{r} at moment t ; $\Phi(\mathbf{r}, \mathbf{\Omega}, t)$ is the density of the photon flux moving in direction $\mathbf{\Omega}$ at point \mathbf{r} at moment t ; $\mu_s(\mathbf{r}, \mathbf{\Omega}' \rightarrow \mathbf{\Omega})$ is the angular differential radiation-scattering coefficient (scattering indicatrix); $\mu(\mathbf{r}) = \mu_a(\mathbf{r}) + \mu_s(\mathbf{r})$ is the extinction factor; $\mu_a(\mathbf{r})$ is the radiation absorption coefficient;

$$\mu_s(\mathbf{r}) = \int_{4\pi} \mu_s(\mathbf{r}, \mathbf{\Omega}' \rightarrow \mathbf{\Omega}) d\Omega' = \int_{4\pi} \mu_s(\mathbf{r}, \mathbf{\Omega}' \rightarrow \mathbf{\Omega}) d\Omega$$

is the radiation scattering coefficient; and v is the absolute value of the radiation propagation velocity in the medium.

In the diffusion approximation, the flux density function $\Phi(\mathbf{r}, \mathbf{\Omega}, t)$ is represented using one scalar $\Phi_d(\mathbf{r}, t)$ and one vector $\mathbf{F}_d(\mathbf{r}, t)$ quantity [7]:

$$\Phi(\mathbf{r}, \mathbf{\Omega}, t) = \Phi_d(\mathbf{r}, t) + \mathbf{F}_d(\mathbf{r}, t) \mathbf{\Omega}. \quad (2)$$

In addition, to obtain a nonstationary diffusion-type equation, supplementary assumptions are needed. In particular, it can be assumed that

$$\left| \frac{1}{v} \frac{\partial}{\partial t} \mathbf{F}_d(\mathbf{r}, t) \right| \ll |\text{grad} \Phi_d(\mathbf{r}, t) + [\mu(\mathbf{r}) - \mu_1(\mathbf{r})] \mathbf{F}_d(\mathbf{r}, t)|. \quad (3)$$

where $\mu_1(\mathbf{r}) = \int_{4\pi} \mathbf{\Omega} \mathbf{\Omega}' \mu_s(\mathbf{r}, \mathbf{\Omega}' \rightarrow \mathbf{\Omega}) d\Omega'$. The quantity $D(\mathbf{r}) = \{3[\mu(\mathbf{r}) - \mu_1(\mathbf{r})]\}^{-1}$ is called the diffusion coefficient.

As is known, the diffusion approximation has a number of serious drawbacks. For example, it poorly describes the behaviour of photons close to the HSM boundaries. In particular, the exact boundary condition, which consists in the fulfilment of the equality $\Phi(\mathbf{r}, \mathbf{\Omega}, t) = 0$ at $\mathbf{n}\mathbf{\Omega} > 0$ at the HSM surface (\mathbf{n} is the vector of the normal to this surface directed into the medium), is not satisfied for this approximation. This boundary condition is most frequently replaced by condition $\int_{\mathbf{n}\mathbf{\Omega} > 0} \Phi(\mathbf{r}, \mathbf{\Omega}, t) (\mathbf{n}\mathbf{\Omega}) d\Omega = 0$. Moreover, the diffusion approximation does not describe ballistic photons and poorly describes the behaviour of photons near radiation sources and inside an HSM in the vicinity of abrupt changes in its characteristics.

The following expression can be derived for the temporal distribution of photons along the axis of a point unidirectional source and a semi-infinite medium [9]:

$$R(z, t) = \frac{1}{2} (4\pi Dv)^{-3/2} t^{-5/2} \exp(-\mu_a vt) \times \left| (z - z_0) \exp\left[-\frac{(z - z_0)^2}{4Dvt}\right] - (z + z_0) \exp\left[-\frac{(z + z_0)^2}{4Dvt}\right] \right|, \quad (4)$$

where $z_0 = (\mu_s - \mu_1)^{-1} = [(1 - g)\mu_s]^{-1}$ and g is the mean cosine of the scattering angle. In this case, the point unidirectional source is replaced by a pair of point isotropic sources (a dipole) separated by a distance $2z_0$. This substitution restricts the layer thickness (it must exceed z_0). We must bear in mind that, if the scattering indicatrix is unknown, it is impossible to precisely determine the mean cosine beforehand.

The nonstationary axial RTE approximation is based on a single assumption concerning the HSM properties – the scattering straight back. In this approximation, it is assumed that each photon is scattered in the direction opposite to its initial motion. In this case, the expression for the scattering indicatrix can be written as [8]

$$\mu_s(\mathbf{r}, \mathbf{\Omega}' \rightarrow \mathbf{\Omega}) = \mu_s(\mathbf{r}) \delta_2(-\mathbf{\Omega}' \mathbf{\Omega}), \quad (5)$$

where $\delta_2(x)$ is the surface delta function and $\mu_s(\mathbf{r})$ is the scattering coefficient in the model of the scattering straight back. In this case, the RTE transforms into a second-order partial differential equation of hyperbolic type, which is much simpler than the initial equation.

In the case of a point unidirectional source and a semi-infinite medium, the expression for the temporal distribution of photons on the optical axis has the form [8]

$$R(z, t) = \eta(\mu vt - \mu z) \frac{v\mu_s z}{[(vt)^2 - z^2]^{1/2}} \times I_1(\mu_s [(vt)^2 - z^2]^{1/2}) \exp(-\mu vt), \quad (6)$$

where $\eta(x)$ is the Heaviside function (the unit step function) and $I_1(x)$ is the modified first-order Bessel function of first kind. The term corresponding to ballistic photons is omitted in (6).

Both models assume that the photon distributions in the cross section with the coordinate z describe the radiation transmitted through a layer with a thickness z . Note that the scattering and absorption coefficients in the axial and diffusion models have somewhat different physical meanings. Their numerical values calculated from the experimental data may correspondingly differ.

An important difference between the axial and diffusion models is that the former imposes limitations only on the medium properties (the scattering indicatrix) but not on the equation form and its solutions; i.e., if the medium properties correspond to the above assumption, the axial model then exactly describes the transmission of radiation through this medium.

Figure 1 shows the main parameters of the temporal distribution of the radiation flux. When studying the transmission of laser pulses through an HSM layer, the simplest method is to vary the layer thickness. Figure 2 shows the shift τ of the distribution peak and its half-width (FWHM) d as functions of thickness z of the scattering layer for the diffusion and axial models. The both models generally yield close results. However, as could be expected, distortions at $z \leq z_0 \sim 1$ mm are present in the diffusion model.

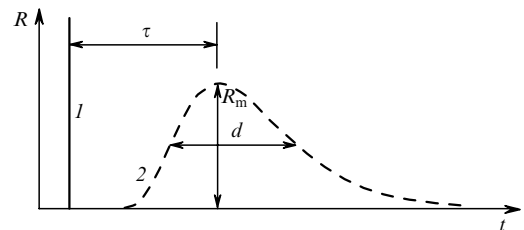


Figure 1. Temporal distribution of an ultrashort pulse transmitted through a scattering medium: (1) ballistic photons and (2) scattered photons. The main parameters of the temporal distribution: the shift τ , the half-width d , and the maximum R_m of the scattered radiation flux.

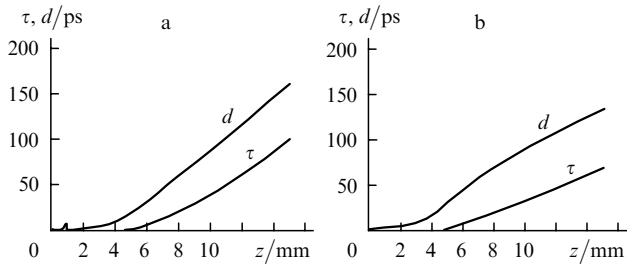


Figure 2. Dependences τ of the distribution maximum and its half-width d on the thickness z of the scattering layer for (a) diffusion and (b) axial models.

3. Experiment

The two models can be compared experimentally in the following manner. Using the temporal distribution measured for a certain thickness of a homogeneous HSM layer, the medium parameters can be found: the extinction and scattering coefficients for the axial model and the absorption and diffusion coefficients for the diffusion model. Then, using the determined values of the medium parameters, one can construct theoretical curves of the photon temporal distribution and superimpose them on the experimental curves. If the theoretical curve is superimposed on the experimental curve which was used to find the medium parameters, the determined parameters then serve as the fitting parameters and can only testify that the theoretical expressions are not senseless. If the medium parameters are found from the experimental curve for one HSM layer thickness (z_1) and the theoretical curve is plotted for another layer thickness (z_2), the comparison of the theoretical curve with the experimental one obtained for thickness z_2 will then demonstrate the prognostic properties of the model, i.e., the accuracy to which this model describes the physical situation.

The experimental data were taken from paper [10], in which experiments with femtosecond laser pulses were described. A laser system consisting of a Ti:sapphire laser and a regenerative amplifier was used. The laser emitted 780-nm, 120-fs pulses with an energy of ~ 0.5 mJ and a pulse repetition rate of 10 Hz. The transmitted radiation was detected with an Imacon-500 image converter camera with a resolution of 1 ps. An aqueous solution of dry milk placed in rectangular glass cells of various thicknesses (1–10 mm) was used as a model HSM.

The medium parameters (for the both models) were determined in the following way [11]. The half-width d and shift τ were determined for the initial experimental curve that corresponded to the initial layer with a certain thickness z_1 . Since there exists a unique combination of the layer thickness, shift, and half-width for the given medium, the curves of constant d and τ values in the $\mu_a - \mu_s$ plane for the axial model and in the $\mu_a - D$ plane for the diffusion model intersect at point A with the coordinates corresponding to the medium parameters (Fig. 3).

The determined parameters were used to construct theoretical temporal distributions for the scattering layer with a thickness z_2 , which could both coincide with z_1 and differ from it. In the latter case, the prognostic properties of the models are studied. The theoretical curves obtained were then superimposed on the experimental curve plotted for the layer with a thickness z_2 (Fig. 4). The ballistic peak whose

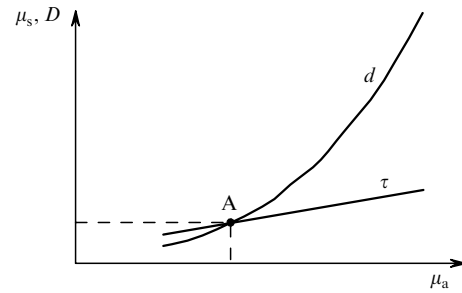


Figure 3. Determination of the medium parameters (point A) from the half-width d and shift τ .

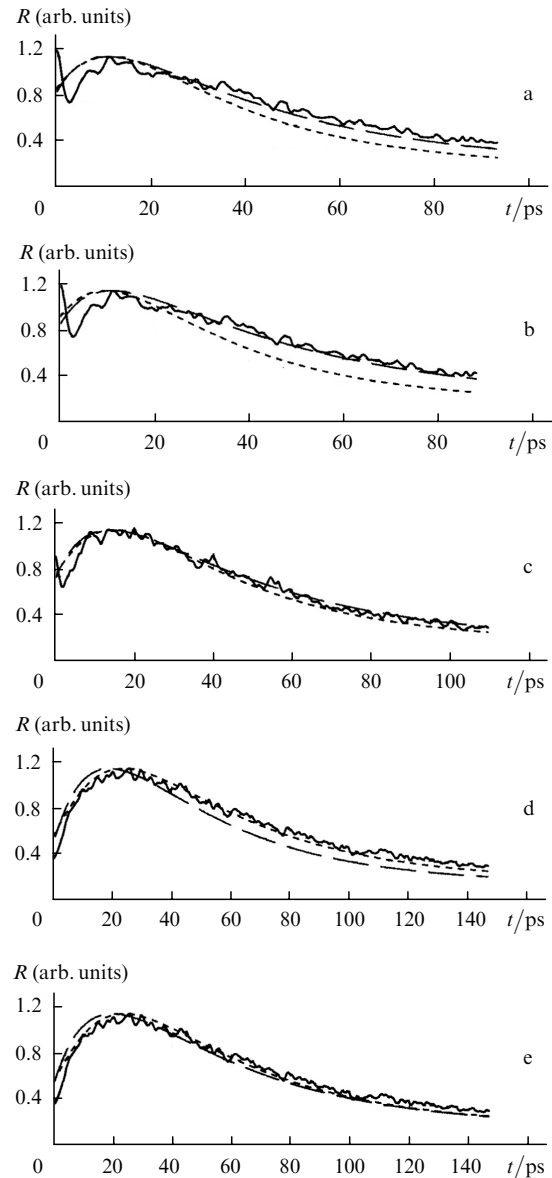


Figure 4. Temporal distributions of photons transmitted through layers of the scattering medium of thickness (a, b) 6.5, (c) 7.0, and (d, e) 8.0 mm. The medium parameters for the models were obtained from the experimental data for layers of thickness (a, c, e) 7.0, (b) 8.0, and (d) 6.5 mm; the experiment, diffusion model, and axial model are plotted with solid lines, short dashes, and long dashes, respectively.

width was determined by the resolution of the image-converter camera was not 'removed' from the experimental curves (Figs 4a, 4b), since it has a weak effect on the rms

Table 1. Comparison of the diffusion and axial models.

| z_1/mm | z_2/mm | Diffusion model | | | | Axial mode | | | |
|-----------------|-----------------|------------------------|------------------------------|---------------|-----------------------|----------------------|------------------------|------------------------|-----------------------|
| | | μ_a/mm^{-1} | $\mu - \mu_1/\text{mm}^{-1}$ | D/mm | σ (arb. units) | μ/mm^{-1} | μ_a/mm^{-1} | μ_s/mm^{-1} | σ (arb. units) |
| 6.0 | 6.0 | 0.003 | 1.15 | 0.29 | 0.28 | 1.15 | 0.09 | 1.06 | 0.30 |
| 6.5 | 6.0 | 0.002 | 1.19 | 0.28 | 0.25 | 1.03 | 0.06 | 0.97 | 0.28 |
| 7.0 | 6.0 | 0.002 | 1.19 | 0.28 | 0.25 | 0.96 | 0.05 | 0.91 | 0.28 |
| 8.0 | 6.0 | 0.002 | 1.15 | 0.29 | 0.26 | 0.93 | 0.04 | 0.89 | 0.28 |
| 6.0 | 6.5 | 0.003 | 1.15 | 0.29 | 0.08 | 1.15 | 0.09 | 1.06 | 0.10 |
| 6.5 | 6.5 | 0.002 | 1.19 | 0.28 | 0.06 | 1.03 | 0.06 | 0.97 | 0.07 |
| 7.0 | 6.5 | 0.002 | 1.19 | 0.28 | 0.06 | 0.96 | 0.05 | 0.91 | 0.07 |
| 8.0 | 6.5 | 0.002 | 1.15 | 0.29 | 0.08 | 0.93 | 0.04 | 0.89 | 0.07 |
| 6.0 | 7.0 | 0.003 | 1.15 | 0.29 | 0.15 | 1.15 | 0.09 | 1.06 | 0.15 |
| 6.5 | 7.0 | 0.002 | 1.19 | 0.28 | 0.13 | 1.03 | 0.06 | 0.97 | 0.12 |
| 7.0 | 7.0 | 0.002 | 1.19 | 0.28 | 0.13 | 0.96 | 0.05 | 0.91 | 0.09 |
| 8.0 | 7.0 | 0.002 | 1.15 | 0.29 | 0.15 | 0.93 | 0.04 | 0.89 | 0.09 |
| 6.0 | 8.0 | 0.003 | 1.15 | 0.29 | 0.09 | 1.15 | 0.09 | 1.06 | 0.16 |
| 6.5 | 8.0 | 0.002 | 1.19 | 0.28 | 0.05 | 1.03 | 0.06 | 0.97 | 0.11 |
| 7.0 | 8.0 | 0.002 | 1.19 | 0.28 | 0.05 | 0.96 | 0.05 | 0.91 | 0.07 |

deviation and was theoretically analysed earlier [12]. The results of our study are listed in Table 1. The rms deviations σ of the models' parameters from the experimental data were calculated for all cases.

4. Conclusions

Although a direct comparison of the medium parameters obtained on the basis of different theoretical models is not quite correct, a certain comparison still can be made. As is expected, the absorption coefficient for the axial model is higher than for the diffusion model, since the photons scattered away from the axis are considered to be absorbed. The diffusion model generally has a low sensitivity to the absorption coefficient. An important fact is that the scattering coefficient for the axial model is close to the difference $\mu - \mu_1$. For small absorption coefficients, this difference is close to the so-called reduced scattering coefficient $\mu'_s = \mu_s - \mu_1 = \mu_s(1 - g)$ in the diffusion model.

The following general conclusions can be made. The theoretical curves plotted for $z_2 = z_1$ are quite precise for the both models. However, the theoretical curves that predict the transmission of radiation through the scattering layer at $z_2 \neq z_1$ differ (sometimes significantly) from the experimental curve. The axial model yields better results at $z_2 < z_1$, and the diffusion model is more precise when the opposite inequality is satisfied. In addition, the axial model is generally preferable for thin layers. Because ballistic photons were not removed from the experimental distributions, their consideration can additionally improve the accuracy of the axial model.

Therefore, despite the fact that the diffusion model is applied much more frequently than the axial model, this study has shown that the latter describes the temporal distributions on the laser axis at least no worse than the diffusion model. Moreover, as was mentioned earlier, the diffusion model is unable in principle to describe ballistic photons, which are especially important for a tomographic reconstruction. Thus, the axial model can be a full-valued alternative to the diffusion model in the field of transmission optical tomography of scattering media.

Acknowledgements. This work was supported in part by the Russian Foundation for Basic Research and the Ministry of Industry and Science of Moscow region (Project Nos 01-01-00065 and 02-02-96000).

References

1. Medical Optical Tomography: Functional Imaging and Monitoring. *Proc. SPIE Int. Soc. Opt. Eng.*, **IS11** (1993).
2. Theoretical Study, Mathematical, Experimental Model for Photon Transport in Scattering Media and Tissue. *Proc. SPIE Int. Soc. Opt. Eng.*, **2326** (1994).
3. Arridge S.R. *Inverse Problems*, **15**, R41 (1999).
4. Podgaetskii V.M., Potapov D.A., Selishchev S.V., Tereshchenko S.A. *Biomed. Tekhnol. Radioelektron.*, **12**, 18 (2001).
5. Case K.M., Zweifel P.F. *Linear Transport Theory* (Reading Mass: Addison-Wesley, 1967; Moscow: Mir, 1972).
6. Kol'chuzhkin A.M., Uchaikin V.V. *Vvedenie v teoriyu prokhozhdeniya chastits cherez veshchestvo* (Introduction to the Theory of Particle Propagation through Matter) (Moscow: Atomizdat, 1978).
7. Ishimaru A. *Wave Propagation and Scattering in Random media* (New York: Academic Press, 1978; Moscow: Mir, 1981) Vol. 1.
8. Selishchev S.V., Tereshchenko S.A. *Zh. Tekh. Fiz.*, **67** (5), 61 (1997).
9. Patterson M.S., Chance B., Wilson B.C. *Appl. Opt.*, **28**, 12 (1989).
10. Podgaetsky V.M., Tereshchenko S.A., Smirnov A.V., Vorob'ev N.S. *Opt. Commun.*, **180**, 217 (2000).
11. Tereshchenko S.A., Podgaetskii V.M., Vorob'ev N.S., Smirnov A.V. *Kvantovaya Elektron.*, **23** (3), 265 (1996) [*Quantum Electron.*, **26** (3), 258 (1996)].
12. Tereshchenko S.A., Podgaetskii V.M., Vorob'ev N.S., Smirnov A.V. *Kvantovaya Elektron.*, **25** (9), 853 (1998) [*Quantum Electron.*, **28** (9), 831 (1998)].